A molecular design strategy to construct the near-infrared fluorescent probe for selectively sensing human cytochrome P450 2J2

Jing Ning,[†,‡,§] Tao Liu,[‡,§] Peipei Dong,[†,§] Wei Wang,[□] Guangbo Ge,[θ] Bo Wang,[†] Zhenlong Yu,[†] Lei Shi,[†] Xiangge Tian,[†] Xiaokui Huo,[†] Lei Feng,[†,‡,*] Chao Wang,[†] Chengpeng Sun,[†] Jingnan Cui,[‡] Tony D. James,[Δ] and Xiaochi Ma[†,*]

[†]College of Integrative Medicine, The National & Local Joint Engineering Research Center for Drug Development of Neurodegenerative Disease, College of Pharmacy, Dalian Medical University, Dalian 116044, China.

[‡]State Key Laboratory of Fine Chemicals, Dalian University of Technology, Dalian 116024, China.

[□]TCM and Ethnomedicine Innovation & Development International Laboratory, Sino-Pakistan TCM and Ethnomedicine Research 8 Center, School of Pharmacy, Hunan University of Chinese Medicine, Changsha 410208, China.

[θ]Institute of Interdisciplinary Integrative Medicine Research, Shanghai University of Traditional Chinese Medicine, Shanghai, 201203, China.

[Δ]Department of Chemistry, University of Bath, Bath BA2 7AY, United Kingdom.

Corresponding authors: Dr. Lei Feng, and Xiaochi Ma, College (Institute) of Integrative Medicine, College of Pharmacy, Dalian Medical University, 9 Western Section, Lvshun South Road, Dalian 116044, China. +86-411-86110419; E-mail: leifeng@mail.dlut.edu.cn (L. Feng); maxc1978@163.com (X. C. Ma).

[§]J. Ning, T. Liu, and P. P. Dong contributed equally.

ABSTRACT

Cytochrome P450 2J2 (CYP2J2), a key enzyme responsible for oxidative metabolism of various xenobiotics and endogenous compounds, participates in a diverse array of physiological and pathological processes in humans. Its biological role in tumorigenesis and cancer diagnosis remains poorly understood, owing to the lack of molecular tools suitable for real-time monitoring CYP2J2 in complex biological systems. Using molecular design principles we were able to modify the distance between the catalytic unit and metabolic recognition moiety, allowing us to develop a CYP2J2 selective fluorescent probe using a near-infrared fluorophore (*E*)-2-(2-(6-hydroxy-2, 3-dihydro-1*H*-xanthen-4-yl)vinyl)-3,3- dimethyl-1-propyl-3*H*-indol-1-ium iodide (**HXPI**). To improve the reactivity and isoform specificity, a self-immolative linker was introduced to the **HXPI** derivatives in order to better fit the narrow substrate channel of CYP2J2, the modification effectively shortened the spatial distance between the metabolic moiety (*O*-alkyl group) and catalytic center of CYP2J2. After screening a panel of *O*-alkylated **HXPI** derivatives, **BnXPI** displayed the best combination of specificity, sensitivity and applicability for detecting CYP2J2 *in vitro* and *in vivo*. Upon *O*-demethylation by CYP2J2, a self-immolative reaction occurred spontaneously *via* 1,6-elimination of *p*-hydroxybenzyl resulting in the release of **HXPI**. Allowing **BnXPI** to be successfully used to monitor CYP2J2 activity in real-time for various living systems including cells, tumor tissues, and tumor-bearing animals. In summary, our practical strategy could help the development of a highly specific and broadly applicable tool for monitoring CYP2J2, which offers great promise for exploring the biological functions of CYP2J2 in tumorigenesis.

Introduction

Cytochrome P450s (CYPs) is part of a superfamily of multifunctional heme-thiolate proteins that play crucial roles in the oxidative metabolism of various xenobiotics and endogenous compounds. CYP2J2, as a key member of the CYPs superfamily, can metabolize endogenous polyunsaturated fatty acids to form vital signaling molecules, resulting in the formation of epoxyeicosatrienoic acids (EETs) and ultimately promotes cell progression.[1] It is mainly expressed in cardiovascular systems including heart and vascular endothelium[2-4] and in a large number of cancers.[5-8] Recently, the available data suggest that high levels of CYP2J2 expression is directly associated with tumorigenesis, and overexpression of CYP2J2 in various carcinoma cell lines (including Tca-8113, A549, Ncl-H446, and HepG2) would promote proliferation and protect the cells against apoptosis. Meanwhile, CYP2J2 was shown to produce several pro-angiogenic lipid products and contribute to metastasis of the tumor by promoting the angiogenesis in and around primary tumors.[6-8] Thus, CYP2J2 could be regarded as a vital biomarker for cancer diagnosis and treatment.

The requirements for the dynamic monitoring of CYP2J2 activity in living systems are strong motivators for the development of novel methods for the detection in various biological systems. Traditional detection methods used for CYP2J2 activity mainly rely upon mass spectrometry or high-performance liquid chromatography,[9,10] which are not suitable for live-specimen evaluation. Fluorescence imaging is an efficient method to simply, safely and sensitively monitor enzymatic activity in cells, tissues and animals, offering high spatiotemporal resolution, noninvasive capability and can be used in living organisms.[11-16] Various enzyme-activatable fluorescent probes have been developed for real-time monitoring enzyme activity and widely utilized in biological research, medical diagnosis and even

intraoperative visualization of various diseases.[17-19] Among the fluorescent probes for sensing protein biomarkers, near-infrared (NIR) imaging reporters have enabled minimization of tissue background fluorescence and light scattering, as well as improvement of photon penetration through deep tissue, thereby providing more accurate imaging or functional evaluation in living systems.[20-25] Thus, activatable NIR fluorescent probe(s) for real-time sensing CYP2J2 activity in living systems are highly desirable, and may facilitate further investigation into the enzymatic functions and diagnosis of the diseases associated with CYP2J2.

However, the development of fluorescent probes for the selective monitoring of target enzymes are a significant challenge, due to the size and shape limits of enzymatic cavities and the complicated substrate recognition process between enzymatic catalytic sites and small molecular fluorophores.[11,26-29] Even if potential fluorophores can enter into the active cavity of the enzyme like a key inserting into a lock, improper spatial distances between the expected metabolic site of the fluorophores and the catalytic center of the target enzyme can seriously restrict the activation of the fluorescent probe by the target enzyme, the analogue being that the key does not open the lock. Therefore, the rational design of a "best-fit" fluorescence molecule to achieve highly effective catalysis towards a target enzyme is essential for success. To solve this challenge, a specific fluorescent probe for CYP2J2 was designed and developed based on the active cavity structure, catalytic characteristic and substrate preference of CYP2J2. To the best of our knowledge, the substrate channel of CYP2J2 is characterized by a cylinder that narrows near the heme prosthetic group, therefore limiting substrate access to the active heme iron for further oxidation.[30,31] Although the active cavity volume for CYP2J2 is similar to that of CYP3A4 (a typical CYP with larger active cavity),[32] CYP2J2 is restricted to the metabolism

of substrates with rigid and bulkier structures.

The great challenge in the design and development of an activatable fluorescent probe for CYP2J2 is how to effectively modify the fluorophore to fit the enzymatic active cavity and adjust the recognition moiety to improve reactivity. Therefore, adjustment of the fluorophore to adapt to the narrow shape of the substrate channel of CYP2J2 is a suitable strategy to facilitate the development of CYP2J2 sensors. In the present study, (*E*)-2-(2-(6-hydroxy-2, 3-dihydro-1*H*-xanthen-4-yl)vinyl)-3,3-dimethyl-1-propyl-3*H*-indol-1-ium iodide (**HXPI**) was selected as the basic fluorophore, as it possesses a long aromatic skeleton and has desirable photophysical properties, excellent tissue penetration, and results in minimal biological damage.[20-25] Meanwhile, we hypothesized that a self-immolative linker (e.g. *p*-hydroxybenzyl group) could be employed as a linker moiety that could adjust the fluorophore to adapt to the structure of CYP2J2 and shorten the spatial distance between the metabolic site of the substrate and the catalytic center of CYP2J2. The metabolic recognition moiety (*O*-alkyl group) of the fluorescence chemosensor was optimized in order to improve the reactivity and isoform-selectivity towards CYP2J2. As expected, upon addition of CYP2J2, the *p*-hydroxybenzyl ether derivatives consistently displayed significantly higher fluorescence response than the corresponding *O*-alkylated **HXPI** derivatives. The self-decomposition of *p*-hydroxybenzyl is triggered by CYP2J2-mediated *O*-demethylation, spontaneously releasing a NIR fluorescence signal. Therefore, by simultaneously optimizing catalytic distance and the metabolic recognition moiety, a highly selective NIR florescence probe of CYP2J2 (**BnXPI**) was successfully developed for the real-time monitoring of endogenous CYP2J2 activity in complex biological systems (Scheme 1). Furthermore, we demonstrated the feasibility and

practicability of the CYP2J2-activatable fluorescent probe for real-time imaging and disease diagnosis, and characterized the potential role played by CYP2J2 in various tumor-associated processes.

RESULTS AND DISCUSSION

Design and synthesis

Currently, the development of an activatable and subtype-selective probe remains a great challenge, due to restricted access of fluorogenic substrates to the active cavity of the target enzyme, resulting in a mismatch of the 'lock-and-key'. Therefore, flexible molecules with conformational flexibility, are recognized and metabolized by CYP2J2. To confirm this assumption, we collected a series of fluorophores possessing either conformational flexibility or rigidity, and their corresponding methylated compounds were designed and synthesized (Figure S1). The *in silico* docking analyses and *in vitro* CYP2J2 incubation assays were performed. As shown in Figure S2 and Table S1, our molecular strategy described above was rational, and comprehensively considers the reactivity, selectivity and fluorescence properties of potential probes for detecting CYP2J2. (*E*)-2-(2-(6-hydroxy-2, 3-dihydro-1*H*-xanthen-4-yl)vinyl)-3,3-dimethyl-1-propyl-3*H*-indol-1-ium iodide (**HXPI**), a well-known NIR dye,[33] was selected as the basic fluorophore with the flexibility suitable for matching CYP2J2. However, probe **1** (**MXPI**, as shown in Scheme 1A), did not fulfill the requirements as a highly-effective substrate of CYP2J2 (namely the key could be inserted into the lock, but it does not open the lock). Therefore, we should optimize this 'key' to obtain the 'best-fit' fluorescent probe that could achieve effective interaction between the metabolic recognition site and catalytic cavity

of CYP2J2.

According to the 3D-structure and metabolic characteristics of CYP2J2, our design strategy was to introduce a self-immolative linker into **HXPI** for improving the catalytic efficiency of dealkylation by shortening the spatial distance between the metabolic recognition moiety (*O*-alkyl group) and the catalytic center of CYP2J2, which will help **HXPI** derivatives adapt to the cylinder and narrow substrate access channel nearby to the heme prosthetic group of CYP2J2 (Scheme 1A). Inspired by the structural characteristic of astemizole, a classical substrate of CYP2J2, with a benzene ring that could facilitate the interaction between ligand and heme of CYP2J2 through π-π stacking (Figure S3), we designed and synthesized a panel of **HXPI** derivatives combining the self-immolative linker (*p*-hydroxybenzyl) along with various alkoxyl groups as the metabolic recognition moieties (Scheme 1B). Our aim was to improve the sensitivity and isoform-specificity for CYP2J2 by adjusting the alkyl groups (such as ethyl, isopropyl, benzyl, etc) on the self-immolative linker. The **HXPI** derivatives could be readily synthesized and their structures were fully characterized by ^{1}H NMR, ^{13}C NMR and HRMS spectra (Scheme S1, Supporting Information). The reactivity and isoform phenotype screening revealed that *O*-alkylated **HXPI** derivatives with self-immolative linkers (probe **5**–**8**) displayed good reactivity towards CYP2J2. In contrast, **HXPI** derivatives without the linker (probe **1**–**4**) could hardly be catalyzed by CYP2J2, and displayed relatively weak fluorescence response and low isoform-specificity. Among all the *p*-hydroxybenzyl ether derivatives, **BnXPI** (probe **5**) gave the highest fluorescence turn-on response towards CYP2J2. The self-decomposition of **BnXPI** is triggered by a CYP2J2-mediated *O*-demethylation that produces a labile linker **HXPI** derivative, and spontaneously produces a strong NIR fluorescence signal. The formation

of **HXPI** mediated by CYP2J2 in the reaction system was confirmed by a comprehensive comparison of LC retention times, UV and MS spectra with standard compounds (Figure S4).

The *in silico* docking analyses elucidated the role of the self-immolative linkers on the catalytic distance, and further verified our design strategy. As shown in Scheme 1B, the spatial distance of the *O*-methyl group of **BnXPI** with the catalytic center of HEME inside the CYP2J2 cavity was calculated as 3.8 Å, which was shorter than that of **MXPI** (5.75 Å). In other words, the catalytic distance of **BnXPI** was effectively shortened by introducing the *p*-hydroxybenzyl ether moiety, which enhanced the catalytic efficiency of CYP2J2 for *O*-demethylation of **HXPI** derivatives. Notably, the π-π stacking interaction between the benzene ring of **BnXPI** and the HEME ring of CYP2J2, as well as the H-bonding interaction between the methoxyl group of **BnXPI** and Thr-315 of CYP2J2, may contribute significantly to the molecular interaction of **BnXPI** with the HEME ring of CYP2J2, all of which indicated that **BnXPI** orients itself markedly better than **MXPI** (probe **1**, without self-immolative linker) in the active site of CYP2J2 (Figure S5 and S6). These results implied that the linker groups on **BnXPI** moved the substrates closer to the catalytic center of CYP2J2, as expected from our design strategy (a key of appropriate length was inserted into the lock, and could turn to open the door). Furthermore, the chemscore value of the bioactive pose of **MXPI** and **BnXPI** in CYP2J2 is -32.71 and -49.31, respectively, which is consistent with the demethylation rate of these two compounds (Table S2). Generally, our molecular design strategy succeeded in optimizing the **HXPI** derivatives to fit the shape of the substrate channel of CYP2J2 by effectively shortening the catalytic distance and adjusting the recognition moieties to achieve an overall 'best-fit' probe. Therefore, our strategy was able to improve the reactivity and selectivity of the fluorescent

probe toward CYP2J2.

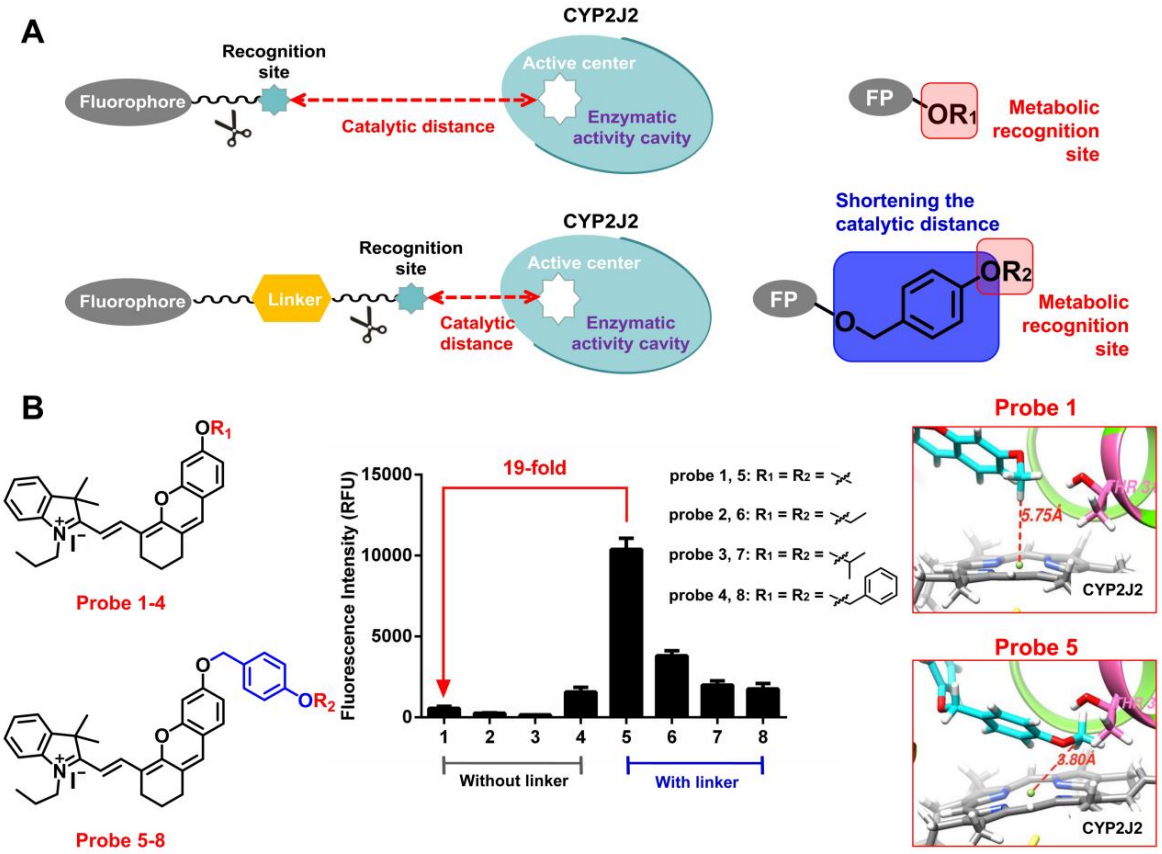

Scheme 1. (A) Design strategy using a self-immolative linker for improving the catalytic rate for CYP2J2. The optimization of the probe was based on adjusting the catalytic distance and recognition moiety. (B) The characteristic structures of *O*-alkoxyl **HXPI** derivatives without (Probe **1**-**4**) or with (Probe **5**-**8**) a *p*-hydroxybenzyl moiety. The fluorescence response of **HXPI** derivatives at 718 nm (λ_{ex} = 656 nm) upon the addition of CYP2J2 for 30 min. Docking simulation of probe **1** (**MXPI**) and probe **5** (**BnXPI**) into CYP2J2, with the catalytic distances shown.

Spectral properties of BnXPI toward CYP2J2

To test the validity of this probe, the spectral properties of **BnXPI** were investigated. Upon addition of CYP2J2, the fluorescence intensity gradually increased at 718 nm (Figure 1). Furthermore, the fluorescence intensity increased linearly when CYP2J2 was progressively

added from 0 to 0.45 mg/mL (R^2 = 0.974). Clearly, the distinct fluorescence response confirmed CYP2J2-mediated dealkylation of **BnXPI** to liberate the oxygen atom as a strong electron donor in the D–π–A structure, thereby increasing the intra-molecular charge transfer (ICT). Upon treatment with CYP2J2, a remarkable change in UV absorption profile of **BnXPI** was also observed, and a color variation from blue to cyan allowed the direct colorimetric detection of CYP2J2 (Figure S7). **BnXPI** was quite stable over a pH range from 7.0 to 12.0, and the pH values did not affect the fluorescence intensity of both **BnXPI** and **HXPI** over this pH range (Figure S8). Together, these results demonstrate that **BnXPI** could be used to detect the CYP2J2 activity under physiological conditions (pH 7.4).

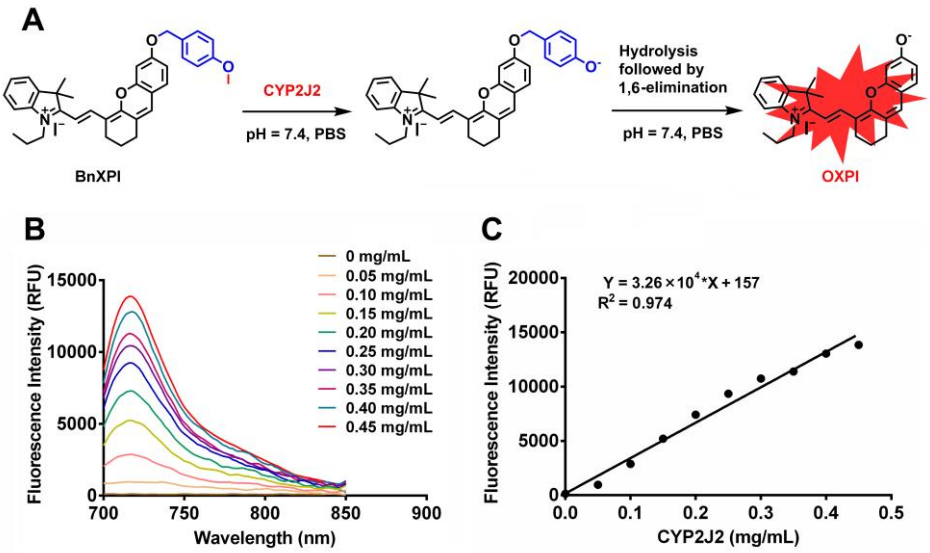

Figure 1. (A) Proposed mechanism of CYP2J2 triggering the fluorescence response of **BnXPI**. (B) Fluorescence spectra of **BnXPI** (10 μM) upon the addition of increasing concentrations of CYP2J2 and incubated for 30 min. λ_{ex} = 656 nm. (C) Fluorescence intensity of **BnXPI** at 718 nm upon the addition of increasing concentrations of CYP2J2 and incubated for 30 min.

Selectivity and sensitivity of BnXPI towards CYP2J2

The selectivity of **BnXPI** was characterized using a panel of CYP isoforms expressed in

various human organs and carcinoma.[5,34-36] It was found that only CYP2J2 could provoke **BnXPI** to generate a significant fluorescence, over other enzymes evaluated (Figure S9). The **HXPI** formation rates of CYP2J2 are 46-fold higher than that of other CYPs. As shown in Figure S10, **BnXPI** exhibited high selectivity for CYP2J2 over the other potential interfering species. Our results indicate that **BnXPI** *O*-demethylation was selectively catalyzed by CYP2J2 even in complex biological matrixes.

The detection limit of **BnXPI** for sensing CYP2J2 was measured as 0.024 mg/mL, indicating the ultra-sensitivity of **BnXPI** to detect CYP2J2 bioactivity (Figure S11). The apparent substrate affinity constant (K_m) value of CYP2J2 for **BnXPI** *O*-demethylation was determined as 4.2 μM (Figure S12). The excellent selectivity and sensitivity of the fluorescence-based assay implied that **BnXPI** enables the rapid and precise detection of CYP2J2 in complex biological samples. Subsequently, a selection of investigations were performed to evaluate the quantitative detection and selective imaging capability of CYP2J2 in biological samples including cancer cells, human tissues and the living model of tumor migration and angiogenesis.

Quantification of CYP2J2 in human tissue microsomes.

The catalytic activities of CYP2J2 in a panel of 13 liver microsomes (HLM) from individual humans are determined (Figure 2A) using **BnXPI**. There was more than 3-fold variation in catalytic activity, which was according to the variation of CYP2J2 protein content in HLM.[37] To verify the ability of **BnXPI** to interact selectively with CYP2J2, the correlation analysis was carried out between the reaction rate of **BnXPI**-*O*-demethylation and the corresponding catalytic activities of CYP2J2, which was determined by a traditional non-florescence based

probe (astemizole, AST). As shown in Figure 2B, the *O*-demethylation rates of **BnXPI** were highly correlated with the metabolic rates of astemizole in these individual HLM.

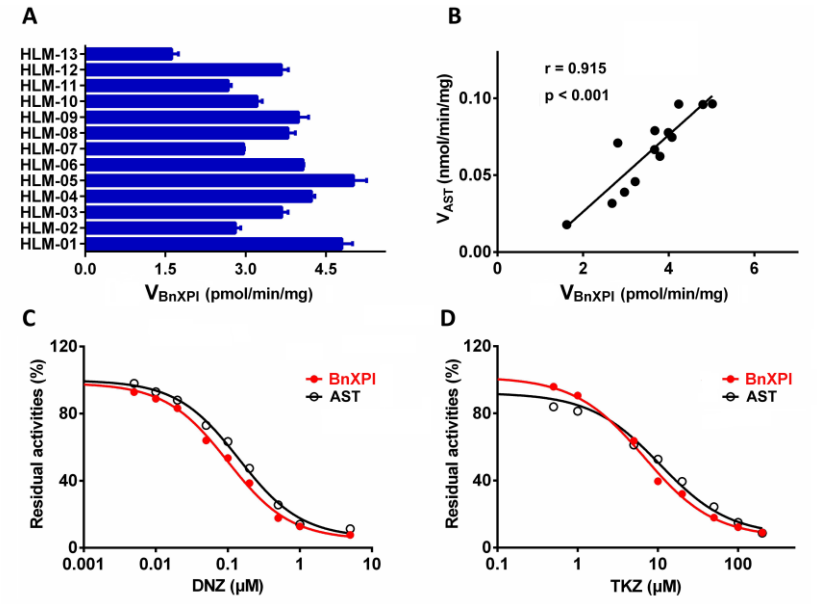

Figure 2. (A) The catalytic activity of CYP2J2 in 13 individual HLM using **BnXPI** as probe substrate. (B) Correlation analysis of metabolic rates of **BnXPI** (10 μM) and AST (10 μM) mediated by CYP2J2. Dose-inhibition curves of danazol (C) and ketoconazole (D) on *O*-demethylation of **BnXPI** and AST.

Recent research has demonstrated the key role of CYP2J2 in the pathogenesis of a variety of human cancers,[5,38] indicating the selective inhibition of CYP2J2 may be a promising therapeutic strategy against cancer.[38,39] In our present work, two known inhibitors of CYP2J2 such as danazol (DNZ) and ketoconazole (TKZ) were used. Their inhibitory effects are similar when using **BnXPI** and the non-florescence based probe astemizole. Indicating that the **BnXPI**-based fluorescence detection method for CYP2J2 activity could be used for the rapid and quantitative measurement of CYP2J2 activities, instead of traditional detection methods (Figure 2C and 2D). These findings suggested that **BnXPI** could serve as a highly selective fluorescent probe for high-throughput screening and accurate characterization of CYP2J2

inhibitors.

Bioimaging in Living Cells.

To demonstrate the potential of **BnXPI** for quantitatively detecting endogenous CYP2J2 activity in intact cells, a variety of human cancer cells from different sources were used as model cells. Prior to biological imaging in living cells, the cell viability of A549 and HepG2 in the presence of **BnXPI** and **HXPI** were evaluated using a standard CCK-8 assay. As shown in Figure S13 and S14, both **BnXPI** and **HXPI** exhibited relatively low toxicity toward the cells examined. **BnXPI** (2.5 μM) was then used for imaging endogenous CYP2J2 in living cells. U251, HepG2, A549 and K562 cells were incubated with **BnXPI** at 37 °C for 1 h and subsequently washed to remove the residual probe. There was a strong fluorescence enhancement for the cells evaluated (Figure 3A). To clarify whether the fluorescence turn-on was triggered by the cellular CYP2J2, chemical inhibition experiments were performed, where cells were treated with DNZ (10 μM) or TKZ (50 μM). As shown in Figure S15, pretreatment with DNZ or TKZ resulted in suppressed fluorescence. The origins of the fluorescence were further confirmed by immunoblot analysis of CYP2J2 protein in cell lysates (Figure 3B and 3C). All the above results proved that the intracellular fluorescence signal could be ascribed to the CYP2J2 mediated activation of **BnXPI**. Collectively, these results confirmed that **BnXPI** can be used to measure endogenous CYP2J2 levels in a variety of cellular contexts.

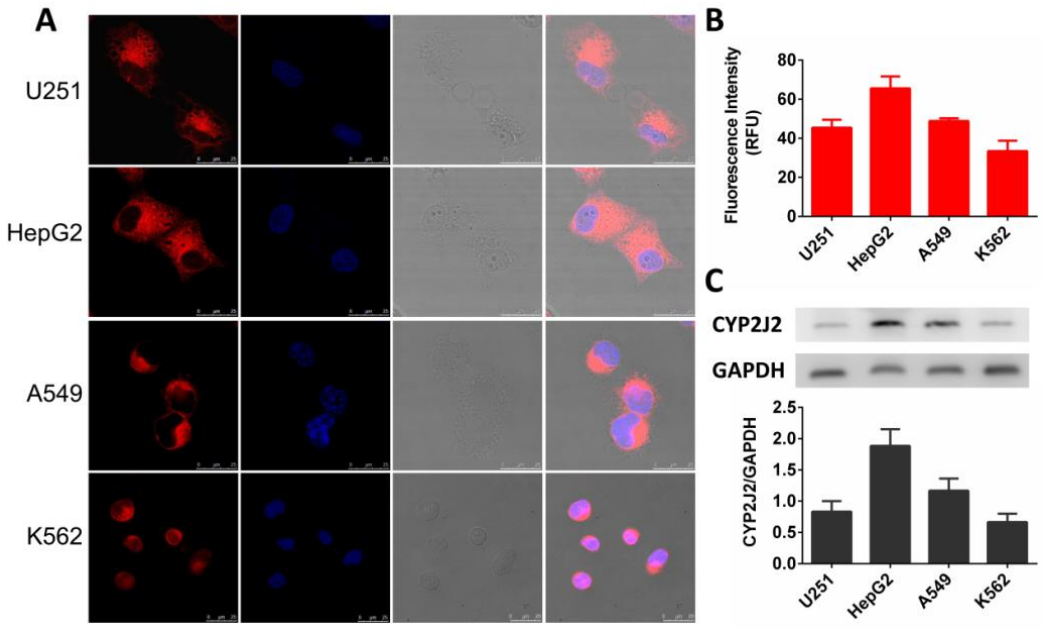

Figure 3. Bioimaging (**A**) and graphical quantification of average fluorescence intensity (**B**) of CYP2J2 activities by **BnXPI** in living human cancer cells. The scale bar is 25 μm. **BnXPI**: excitation, 633 nm; semiconductor laser emission, 690−750 nm. (C) The protein level of CYP2J2 in tumor cells was analyzed by western blot using glyceraldehyde-3-phosphate dehydrogenase (GAPDH) as an internal reference.

Given migration is regarded as the core hallmark of cancer manifesting with malignant transformation ability, the potential role of CYP2J2 on migration was investigated. We detected the consequences of silencing CYP2J2 on A549 cell motility as well as **BnXPI** imaging performance during this biological process. After pretreating with siRNA, A549 cells exhibited a suppressed fluorescence signal, which was in agreement with the markedly reduced protein level of CYP2J2 (Figure S16). As shown in Figure S17, the migration ability of CYP2J2 silenced cells was impaired so that the scraped space was not occupied by cells. These results demonstrate the application of **BnXPI** for tumor cell analysis, such as migration assay. Furthermore, these results imply that CYP2J2 plays an important role in the acceleration of cancer migration, while its inhibition may be a promising anti-cancer therapeutic approach.

Bioimaging of angiogenesis by BnXPI *in vitro* and *ex vivo*

Angiogenesis plays a vital role in the growth and spread of cancer, given that an adequate blood supply is necessary for tumor growth and invasion into normal tissue.[40,41] CYP2J2 is a key enzyme responsible for the conversion of arachidonic acid to pro-angiogenic epoxy metabolite EETs. Therefore, the biological function of CYP2J2 in carcinogenesis has attracted significant attention.[42-45] Inspired by the high expression of CYP2J2 in vascular endothelial cells,[2-4] we examined the capability of **BnXPI** for the visualization of human umbilical vein endothelial cells (HUVEC) and monitoring the neovessel formation in the constructed angiogenesis models. As expected, a strong fluorescence enhancement was observed in HUVEC after incubation with **BnXPI**. Furthermore, HUVEC pretreated with CYP2J2 selective inhibitors (danazol or ketoconazole) or CYP2J2 siRNA, exhibited a significantly suppressed fluorescence signal (Figure S18 and S19). We then evaluated an *in vitro* tube formation angiogenesis model. **BnXPI** can clearly indicate tubular morphogenesis of HUVEC (Figure 4A-i), and the migration and tube-forming ability of cells that were pretreated with CYP2J2 siRNA or inhibitors was significantly impaired (Figure 4A-iii, v, vii, ix). It should be noted that the correlation between CYP2J2 activity and HUVEC migration was visualized using CYP2J2 activatable sensor (**BnXPI**). Subsequently, the capacity of **BnXPI** for monitoring the neovessel formation was verified by a 3D spheroid sprouting and an *ex vivo* neonatal ventricle culture assay.[46] We found that **BnXPI** could precisely elucidate neovessels sprouted from 3D spheroid sprouting (Figure 4B) and the heart tissues (Figure 4C). These results indicate that **BnXPI** can provide a NIR readout for the *in situ* quantitative tracking of endogenous CYP2J2 activity and visualization of neovessels in an angiogenesis model. Notably, the down regulation of CYP2J2 by siRNA as

well as inhibition of CYP2J2 activity by chemical inhibitors could effectively inhibit the tube-formation of endothelial cells. We believe that the 3D visible method of angiogenesis using **BnXPI** could lead to an explosion of research to discover novel CYP2J2 mediators-induced anti-angiogenesis therapeutics.

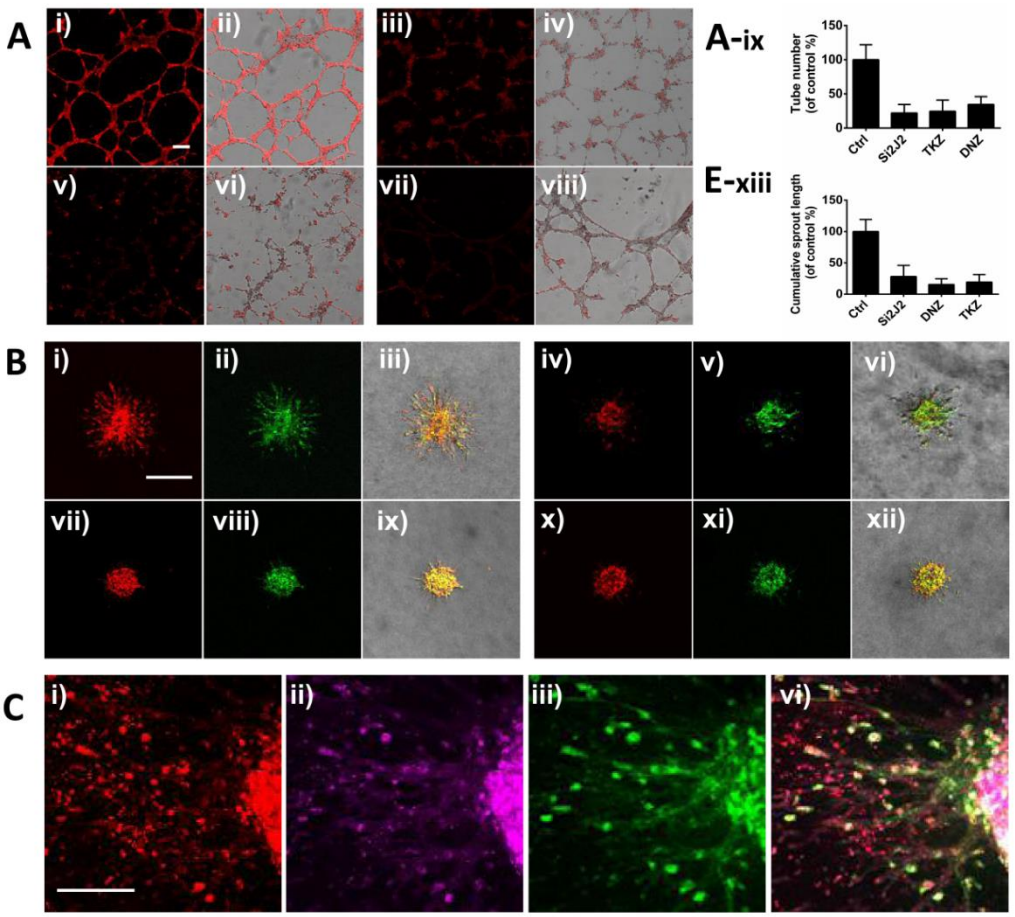

Figure 4. Bioimaging of angiogenesis using **BnXPI** *in vivo* and *ex vivo*. (A) Confocal fluorescence imaging of tube formation in matrigel angiogenesis assay. Images of endothelial cell tube (i-ii), CYP2J2 knockdown cell tube (iii-iv), TKZ (v-vi) or DNZ (vii-viii) pretreated cell tube. (B) Imaging of endothelial cell spheroids. Cell spheroids were pretreated with siRNA (iv-vi), TKZ (vii-ix) or DNZ (x-xii). (C) Imaging of endothelial cell sprouting from three-dimensional heart angiogenesis assay. **BnXPI** (red), immunofluorescence for CYP2J2 (pink), FITC-Lectin (green). Scale bar is 250 μm.

Bioimaging by BnXPI in bio-specimens of clinical patients with haematological

malignancies

We then examined whether CYP2J2 activity in peripheral blood white cells can be detected using **BnXPI**, aiming to develop a diagnostic tool for human haematologic malignancies.[47-50] For this purpose, we set out to examine whether **BnXPI** could detect CYP2J2 activities in six samples of peripheral blood collected from different patients with leukemia and lymphoma. The detailed clinical data and CYP2J2 expression of patients is given in Figure S20 and Table S3. We succeeded in detecting CYP2J2 activity in peripheral blood white cells from patients (Figure 5A). Furthermore, the fluorescence signal verified by flow cytometry, was directly proportional to the CYP2J2 expression measured by western blot (Figure 5B and 5C). The very weak fluorescence emission of **HXPI** in samples of healthy volunteers are attributed to the low protein levels of CYP2J2 in normal peripheral blood, which agrees with previous research.[48] Subsequently, **BnXPI** was tentatively used as a prognostic indicator for acute myeloid leukeamia. The dramatic rise of immature stem cells and myeloblasts in the plasma of patients with acute myeloid leukeamia was effectively elucidated by **BnXPI**-based imaging assisted by CD34 and CD117 analysis (Figure S21). Thus, we performed the real-time imaging of the abnormal surplus of white cells in peripheral blood using **BnXPI**, which provided some important information for the diagnosis, classification and monitoring of hematological malignancies.

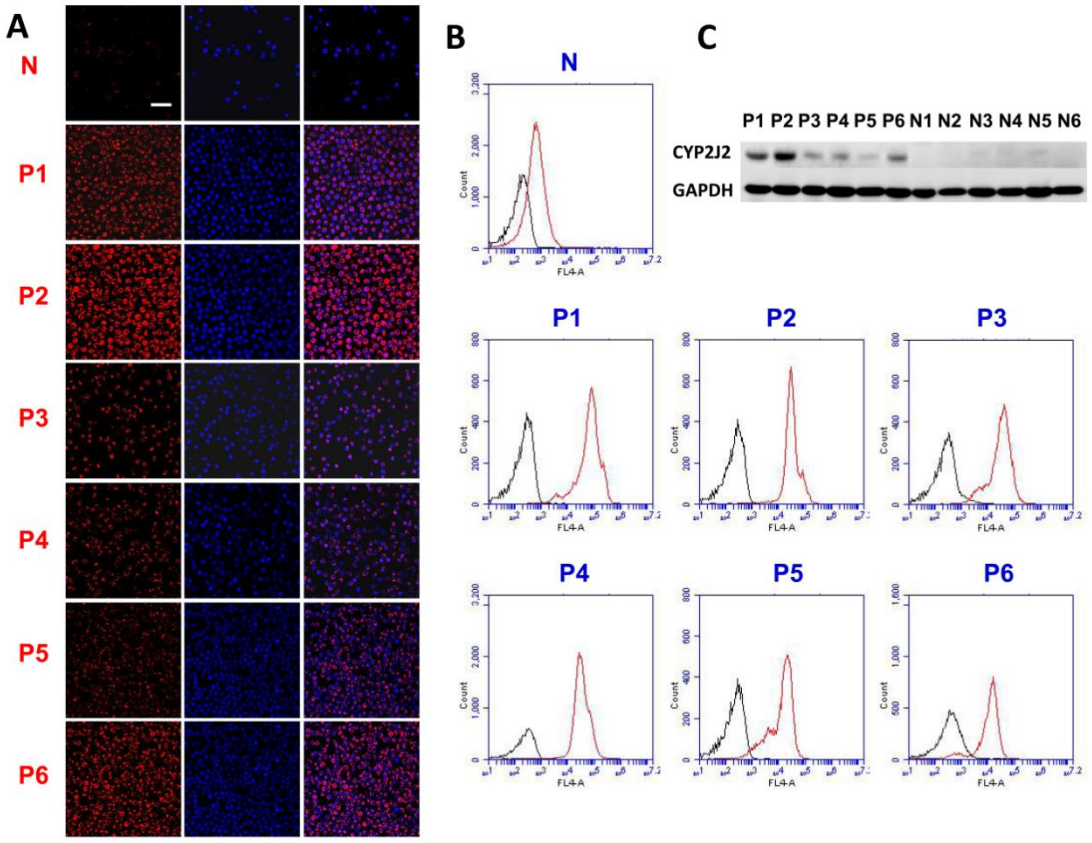

Figure 5. Confocal fluorescence imaging (A) and flow cytometric analyses (B) of CYP2J2 activities in peripheral white blood cells from healthy volunteers (N1-N6) and patients with leukemia or lymphoma (P1-P6). Scale bar is 50 μm. (C) Protein level of CYP2J2 in peripheral white blood cells analyzed by western blot using GAPDH as an internal reference.

Real-time *In Vivo* Imaging of CYP2J2 Activity in Tumors

Inspired by the distinct 'light-up' NIR emission, we examined the capability of **BnXPI** for real-time *in vivo* visualization of CYP2J2 activity of tumors. Owing to amplified fluorescence by enzymatic turnover and particularly low background interference in the NIR region, a NIR fluorescent signal was observed rapidly in the tumor region after injection of **BnXPI** into the tumor (Figure 6A). It should be noted that, just after 10 min post injection, the NIR fluorescence signal was observed and had spread to the whole tumor region, indicative of the rapid activation and high sensitivity of **BnXPI** for CYP2J2. The fluorescence intensity gradually increased,

reaching a maximum level after 1 h post injection, and then slowly decayed over time. We further recorded the *ex vivo* fluorescence images of tumor and adjacent normal tissue collected immediately after sacrificing the mice, and the adjacent tissues of cancer displayed no fluorescence signal (Figure 6B). The imaging of CYP2J2 in tumor tissue sections after staining with **BnXPI** was preformed upon excitation at 633 nm, and the remarkable fluorescence image induced by CYP2J2 is in good accordance with the immunohistochemical staining with CYP2J2 antibodies. Additionally, excellent results were also observed for the imaging of human tumor sections (Figure S22). Taken together, these findings indicate that **BnXPI** is a useful molecular tool for imaging CYP2J2 in tumors and tissue sections, which could be used for surgical diagnosis and therapy of cancers in clinics.

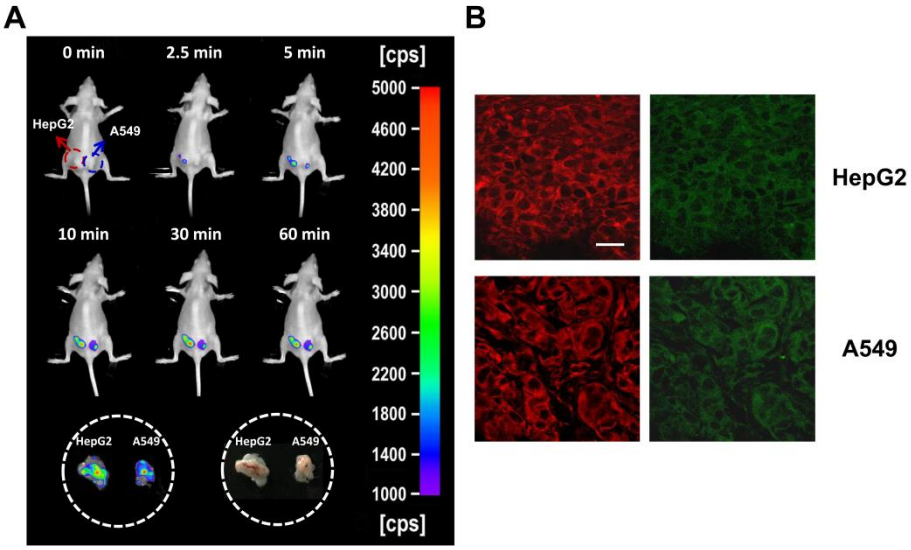

Figure 6. (A) *In vivo* NIR fluorescence imaging of CYP2J2 in tumor-bearing nude mice after tumor injection. The grown tumor tissue was taken from the mouse. (B) Fluorescence (left) and immunofluorescence (right) images of the CYP2J2 in tumor tissue slice. Scale bar is 50 μm. **BnXPI** (red): excitation, 633 nm; semiconductor laser emission collected, 690−750 nm. Immunofluorescence for CYP2J2 (green): excitation, 543 nm; emission collected, 590−650 nm.

CONCLUSION

Using a structure-based molecular design strategy, we have successfully developed the first near-infrared (NIR) activatable fluorescent probe for the selective and real-time detection of CYP2J2. According to the structural features and substrate preference of CYP2J2, a dealkylation-based trigger utilizing a self-immolative linker attached to **HXPI**, was critical in facilitating the excellent "Lock and Key" fit, in order to facilitate the *O*-dealkylation of **HXPI** derivatives. After screening and optimization, **BnXPI** displayed the ideal combination of selectivity, sensitivity and NIR fluorescence response following CYP2J2-mediated *O*-demethylation. **BnXPI** could be specifically activated in various cancer cells and the neovessels of endothelial cells, thereby providing a light-up readout for the quantitative tracking of endogenous CYP2J2 activity and visualization of the angiogenesis process. Furthermore, **BnXPI** has been successfully applied for the real-time imaging of CYP2J2 in tumor-bearing mice. In summary, a new NIR fluorescence based probe **BnXPI** has been developed and fully characterized for sensitive detection of CYP2J2, which holds great promise for CYP2J2-associated carcinoma diagnosis and treatment, and for further investigations into the potential biological functions of CYP2J2. Furthermore, our practical strategy facilitates a new route for developing enzyme-activatable and isoform-specific fluorescent probes for target enzymes.

ASSOCIATED CONTENT

Supporting information

More detailed experimental procedures, characterizations, supplementary optical spectra and figures can be found in Supporting Information.

AUTHOR INFORMATION

Corresponding Author

leifeng@mail.dlut.edu.cn (L. Feng); maxc1978@163.com (X. C. Ma)

Author Contributions

§ J. Ning, T. Liu, and P. P. Dong contributed equally.

NOTES

The authors declare no competing financial interest.

ACKNOWLEDGMENTS

The authors thank the National Natural Science Foundation of China (81622047, 81503201, 81473334 and 21572029), the Distinguished Professor of Liaoning Province program and State Key Laboratory of Fine Chemicals (KF1603) for financial support. TDJ wishes to thank the Royal Society for a Wolfson Research Merit Award.

REFERENCES

(1) Pozzi, A.; Macias-Perez, I.; Abair, T.; Wei, S.; Su, Y.; Zent, R.; Falck, J. R.; Capdevila, J. H. Characterization of 5,6- and 8,9-epoxyeicosatrienoic acids (5,6- and 8,9-EET) as potent in vivo angiogenic lipids. *J. Biol. Chem.* **2005**, *280*, 27138-27146.

(2) Node, K.; Huo, Y.; Ruan, X.; Yang, B.; Spiecker, M.; Ley, K.; Zeldin, D. C.; Liao, J. K. Anti-inflammatory properties of cytochrome P450 epoxygenase-derived eicosanoids. *Science* **1999**, *285*, 1276-1279.

(3) Imig, J. D. Epoxides and soluble epoxide hydrolase in cardiovascular physiology. *Physiol. Rev.* **2012**, *92*, 101-130.

(4) Askari, A.; Thomson, S. J.; Edin, M. L.; Zeldin, D. C.; Bishop-Bailey, D. Roles of the

epoxygenase CYP2J2 in the endothelium. *Prostaglandins Other Lipid Mediat.* **2013**, *107*, 56-63.

(5) Jiang, J. G.; Chen, C. L.; Card, J. W.; Yang, S.; Chen, J. X.; Fu, X. N.; Ning, Y. G.; Xiao, X.; Zeldin, D. C.; Wang, D. W. Cytochrome P450 2J2 promotes the neoplastic phenotype of carcinoma cells and is up-regulated in human tumors. *Cancer Res.* **2005**, *65*, 4707-4715.

(6) Jiang, J. G.; Ning, Y. G.; Chen, C.; Ma, D.; Liu, Z. J.; Yang, S.; Zhou, J.; Xiao, X.; Zhang, X. A.; Edin, M. L.; Card, J. W.; Wang, J.; Zeldin, D. C.; Wang, D. W. Cytochrome p450 epoxygenase promotes human cancer metastasis. *Cancer Res.* **2007**, *67*, 6665-6674.

(7) Panigrahy, D.; Edin, M. L.; Lee, C. R.; Huang, S.; Bielenberg, D. R.; Butterfield, C. E.; Barnés, C. M.; Mammoto, A.; Mammoto, T.; Luria, A.; Benny, O.; Chaponis, D. M.; Dudley, A. C.; Greene, E. R.; Vergilio, J. A.; Pietramaggiori, G.; Scherer-Pietramaggiori, S. S.; Short, S. M.; Seth, M.; Lih, F. B.; Tomer, K. B.; Yang, J.; Schwendener, R. A.; Hammock, B. D.; Falck, J. R.; Manthati, V. L.; Ingber, D. E.; Kaipainen, A.; D'Amore, P. A.; Kieran, M. W.; Zeldin, D. C. Epoxyeicosanoids stimulate multiorgan metastasis and tumor dormancy escape in mice. *J. Clin. Invest.* **2012**, *122*, 178-191.

(8) Karkhanis, A.; Hong, Y.; Chan, E. C. Y. Inhibition and inactivation of human CYP2J2: Implications in cardiac pathophysiology and opportunities in cancer therapy. *Biochem. Pharmacol.* **2017**, *135*, 12-21.

(9) Matsumoto, S.; Yamazoe, Y. Involvement of multiple human cytochromes P450 in the liver microsomal metabolism of astemizole and a comparison with terfenadine. *Br. J. Clin. Pharmacol.* **2001**, *51*, 133-142.

(10) Lee, C. A.; Jones, J. P. 3rd.; Katayama, J.; Kaspera, R.; Jiang, Y.; Freiwald, S.; Smith, E.; Walker, G. S.; Totah, R. A. Identifying a selective substrate and inhibitor pair for the evaluation of CYP2J2 activity. *Drug Metab. Dispos.* **2012**, *40*, 943-956.

(11) Zhang, H.; Fan, J.; Wang, J.; Zhang, S.; Dou, B.; Peng, X. An off-on COX-2-specific fluorescent probe: targeting the Golgi apparatus of cancer cells. *J. Am. Chem. Soc.* **2013**, *135*, 11663-11669.

(12) Lee, M. H., Park, N., Yi, C., Han, J. H., Hong, J. H., Kim, K. P., Kang, D. H,, Sessler, J. L., Kang, C., Kim, J. S. Mitochondria-immobilized pH-sensitive off-on fluorescent probe. *J. Am. Chem. Soc.* **2014**, *136*, 14136-14142.

(13) Guo, Z.; Park, S.; Yoon, J.; Shin, I. Recent progress in the development of near-infrared fluorescent probes for bioimaging applications. *Chem. Soc. Rev.* **2014**, *43*, 16-29.

(14) Zhou, L.; Zhang, X.;Wang, Q.; Lv, Y.; Mao, G.; Luo, A.; Wu, Y.; Wu, Y.; Zhang, J.; Tan, W. Molecular engineering of a TBET-based two-photon fluorescent probe for ratiometric imaging of living cells and tissues. *J. Am. Chem. Soc.* **2014**, *136*, 9838-9841.

(15) Gong, Q.; Shi, W.; Li, L.; Wu, X.; Ma, H. Ultrasensitive Fluorescent Probes Reveal an Adverse Action of Dipeptide Peptidase IV and Fibroblast Activation Protein during Proliferation of Cancer Cells. *Anal. Chem.* **2016**, *88*, 8309-8314.

(16) Yan, J.; Lee, S.; Zhang, A.; Yoon, J. Self-immolative colorimetric, fluorescent and chemiluminescent chemosensors. *Chem. Soc. Rev.* **2018**, *47*, 6900-6916.

(17) Liu, T.; Ning, J.; Wang, B.; Dong, B.; Li, S.; Tian, X.; Yu, Z.; Peng, Y.; Wang, C.; Zhao, X.; Huo, X.; Sun, C.; Cui, J.; Feng, L.; Ma, X. Activatable Near-Infrared Fluorescent Probe for Dipeptidyl Peptidase IV and Its Bioimaging Applications in Living Cells and Animals. *Anal. Chem.* **2018**, *90*, 3965-3973.

(18) Liu, H. W.; Chen, L. L.; Xu, C. Y.; Li, Z.; Zhang, H. Y.; Zhang, X. B.; Tan, W. H. Recent progresses in small-molecule enzymatic fluorescent probes for cancer imaging. *Chem. Soc. Rev.* **2018**, *47*, 7140-7180.

(19) Zhang, J. J., Chai X. Z., He X. P., Kim, H. J., Yoon, J. Y., Tian, H. Fluorogenic probes for disease-relevant enzymes. *Chem. Soc. Rev.* **2018**, DOI: 10.1039/c7cs00907k.

(20) Li, L.; Li, Z.; Shi, W.; Li, X.; Ma, H. Sensitive and selective near-infrared fluorescent off-on probe and its application to imaging different levels of β-lactamase in Staphylococcus aureus. *Anal. Chem.* **2014**, *86*, 6115-6120.

(21) Yuan, L.; Lin, W.; Zhao, S.; Gao, W.; Chen, B.; He, L.; Zhu, S. A unique approach to development of near-infrared fluorescent sensors for in vivo imaging. *J. Am. Chem. Soc.* **2012**, *134*, 13510-13523.

(22) Wan, Q.; Chen, S.; Shi, W.; Li, L.; Ma, H. Lysosomal pH rise during heat shock monitored by a lysosome-targeting near-infrared ratiometric fluorescent probe. *Angew Chem. Int Ed. Engl.* **2014**, *53*, 10916-10920.

(23) Wrobel, A. T.; Johnstone, T. C.; Deliz Liang A.; Lippard, S. J.; Rivera-Fuentes, P. A fast and selective near-infrared fluorescent sensor for multicolor imaging of biological nitroxyl

(HNO). *J. Am. Chem. Soc.* **2014**, *136*, 4697-4705.

(24) He, X.; Li, L.; Fang, Y.; Shi, W.; Li, X.; Ma, H. In vivo imaging of leucine aminopeptidase activity in drug-induced liver injury and liver cancer via a near-infrared fluorescent probe. *Chem. Sci.* **2017**, *8*, 3479-3483.

(25) Li, H.; Li, X.; Shi, W.; Xu, Y.; Ma, H. Rationally Designed Fluorescence •OH Probe with High Sensitivity and Selectivity for Monitoring the Generation of •OH in Iron Autoxidation without Addition of H_2O_2. *Angew. Chem. Int. Ed.* **2018**, *57*, 12830 -12834.

(26) Dai, Z. R.; Ge, G. B.; Feng, L.; Ning, J.; Hu, L. H.; Jin, Q.; Wang, D. D.; Lv, X.; Dou, T. Y.; Cui, J. N.; Yang, L. A Highly Selective Ratiometric Two-Photon Fluorescent Probe for Human Cytochrome P450 1A. *J. Am. Chem. Soc.* **2015**, *137*, 14488-14495.

(27) Wu, X.; Li, L.; Shi, W.; Gong, Q.; Ma, H. Near-Infrared Fluorescent Probe with New Recognition Moiety for Specific Detection of Tyrosinase Activity: Design, Synthesis, and Application in Living Cells and Zebrafish. *Angew Chem. Int. Ed. Engl.* **2016**, *55*, 14728-14732.

(28) Ning, J.; Tian, Z. H.; Wang, B.; Ge, G. B.; An, Y.; Hou, J.; Wang, C.; Zhao, X. Y.; Li, Y. N.; Tian, X. G.; Yu, Z. L.; Huo, X. K.; Sun, C. P.; Feng, L.; Cui, J. N.; Ma, X. C. A highly sensitive and selective two-photon fluorescent probe for real-time sensing of cytochrome P450 1A1 in living systems. *Mater. Chem. Front.* **2018**, *2*, 2013-2020.

(29) Wu, X.; Shi, W.; Li, X.; Ma, H. A Strategy for Specific Fluorescence Imaging of Monoamine Oxidase A in Living Cells. *Angew. Chem. Int. Ed. Engl.* **2017**, *56*, 15319-15323.

(30) Lafite, P.; André, F.; Zeldin, D. C.; Dansette, P. M.; Mansuy, D. Unusual regioselectivity and active site topology of human cytochrome P450 2J2. *Biochemistry* **2007**, *46*, 10237-10247.

(31) Lee, C. A.; Neul, D.; Clouser-Roche, A.; Dalvie, D.; Wester, M. R.; Jiang, Y.; Jones, J. P. 3rd; Freiwald, S.; Zientek, M.; Totah, R. A. Identification of novel substrates for human cytochrome P450 2J2. *Drug Metab. Dispos.* **2010**, *38*, 347-356.

(32) Gay, S. C.; Roberts, A. G.; Halpert, J. R. Structural features of cytochromes P450 and ligands that affect drug metabolism as revealed by X-ray crystallography and NMR. *Future Med. Chem.* **2010**, *2*, 1451-1468.

(33) Jin, Y.; Tian, X.; Jin, L.; Cui, Y.; Liu, T.; Yu, Z.; Huo, X.; Cui, J.; Sun, C.; Wang, C.; Ning, J.; Zhang, B.; Feng, L.; Ma, X. Highly Specific near-Infrared Fluorescent Probe for the Real-Time Detection of β-Glucuronidase in Various Living Cells and Animals. *Anal. Chem.* **2018**,

90, 3276-3283.

(34) Wei, P.; Zhang, J.; Egan-Hafley, M.; Liang, S.; Moore, D. D. The nuclear receptor CAR mediates specific xenobiotic induction of drug metabolism. *Nature* **2000**, *407*, 920-923.

(35) Murray, G. I. The role of cytochrome P450 in tumour development and progression and its potential in therapy. *J. Pathol.* **2000**, *192*, 419-426.

(36) Enayetallah, A. E.; French, R. A.; Grant, D. F. Distribution of soluble epoxide hydrolase, cytochrome P450 2C8, 2C9 and 2J2 in human malignant neoplasms. *J. Mol. Histol.* **2006**, *37*, 133-141.

(37) Yamazaki, H.; Okayama, A.; Imai, N.; Guengerich, F. P.; Shimizu, M. Inter-individual variation of cytochrome P4502J2 expression and catalytic activities in liver microsomes from Japanese and Caucasian populations. *Xenobiotica* **2006**, *36*, 1201-1209.

(38) Chen, C.; Li, G.; Liao, W.; Wu, J.; Liu, L.; Ma, D.; Zhou, J.; Elbekai, R. H.; Edin, M. L.; Zeldin, D. C.; Wang, D. W. Selective inhibitors of CYP2J2 related to terfenadine exhibit strong activity against human cancers in vitro and in vivo. *J. Pharmacol. Exp. Ther.* **2009**, *329*, 908-918.

(39) Lee, B.; Wu, Z.; Sung, S. H.; Lee, T.; Song, K. S.; Lee, M. Y.; Liu, K. H. Potential of decursin to inhibit the human cytochrome P450 2J2 isoform. *Food Chem. Toxicol.* **2014**, *70*, 94-99.

(40) Folkman, J. Angiogenesis in cancer, vascular, rheumatoid and other disease. *Nat. Med.* **1995**, *1*, 27-31.

(41) Carmeliet, P.; Jain, R. K. Angiogenesis in cancer and other diseases. *Nature* **2000**, *407*, 249-257.

(42) Node, K.; Huo, Y.; Ruan, X.; Yang, B.; Spiecker, M.; Ley, K.; Zeldin, D. C.; Liao, J, K. Anti-inflammatory properties of cytochrome P450 epoxygenase-derived eicosanoids. *Science* **1999**, *285*, 1276-1279.

(43) Turner, H. E.; Harris, A. L.; Melmed, S.; Wass, J. A. Angiogenesis in endocrine tumors. *Endocrine reviews.* **2003**, *24*, 600-632.

(44) Zhao, Y.; Adjei, A. A. Targeting Angiogenesis in Cancer Therapy: Moving Beyond Vascular Endothelial Growth Factor. *Oncologist* **2015**, *20*, 660-673.

(45) Shojaei, F. Anti-angiogenesis therapy in cancer: current challenges and future perspectives.

Cancer Lett. **2012**, *320*, 130-137.

(46) Kiefer, F. N.; Munk, V. C.; Humar, R.; Dieterle, T.; Landmann, L.; Battegay, E. J. A versatile in vitro assay for investigating angiogenesis of the heart. *Exp. Cell. Res.* **2004**, *300*, 272-282.

(47) Allemani, C.; Matsuda, T.; Di Carlo, V.; Harewood, R.; Matz, M.; Nikšić, M.; Bonaventure, A.; Valkov, M.; Johnson, C. J.; Estève, J.; Ogunbiyi, O. J.; Azevedo E Silva, G.; Chen, W. Q.; Eser, S.; Engholm, G.; Stiller, C. A.; Monnereau, A.; Woods, R. R.; Visser, O.; Lim, G. H.; Aitken, J.; Weir, H. K.; Coleman, M. P.; CONCORD Working Group. Global surveillance of trends in cancer survival 2000-14 (CONCORD-3): analysis of individual records for 37 513 025 patients diagnosed with one of 18 cancers from 322 population-based registries in 71 countries. *Lancet* **2018**, *391*, 1023-1075.

(48) Chen, C.; Wei, X.; Rao, X.; Wu, J.; Yang, S.; Chen, F.; Ma, D.; Zhou, J.; Dackor, R. T.; Zeldin, D. C.; Wang, D. W. Cytochrome P450 2J2 is highly expressed in hematologic malignant diseases and promotes tumor cell growth. *J. Pharmacol. Exp. Ther.* **2011**, *336*, 344-355.

(49) El-Serafi, I.; Fares, M.; Abedi-Valugerdi, M.; Afsharian, P.; Moshfegh, A.; Terelius, Y.; Potácová, Z.; Hassan, M. Cytochrome P450 2J2, a new key enzyme in cyclophosphamide bioactivation and a potential biomarker for hematological malignancies. *Pharmacogenomics J.* **2015**, *15*, 405-413.

(50) Raccor, B. S.; Kaspera, R. Extra-hepatic isozymes from the CYP1 and CYP2 families as potential chemotherapeutic targets. *Curr. Top Med. Chem.* **2013**, *13*, 1441-1453.